Dark matter and Dark Energy should be identified by the 3-Cosmic Framework of String Theory

Hsien-Jung Ho
Host / Newidea Research Center
ORCID ID: 0009-0006-9330-7002
e-mail: newidea@newidea.org.tw
Address: 10 Floor, No. 110-6, Jie-Shou N Road, Changhua City, Taiwan.

ABSTRACT

Based on the ten-dimensional spacetime described in original string theory, the Anthropic Principle and Causality are applied to the structure of space and time, allowing the Universe to be divided into three distinct cosmoses, which means a 3-cosmic framework of the Universe. According to the string theory, between any two cosmoses, except gravitational force, there is no other fundament force that implying dark matter in cosmoses other than ours. By applying geophysics to analyze the Earth's interior and using a simplification method to calculate the data of a new Earth model, a dark planet has been figured out — approximately 1.33 times the mass of Mars — located inside the Earth, but existing in a different cosmos other than ours. Using cosmological parameter data ranging from the 1-year WMAP results to the Planck satellite 2018 results, the dark energy has gradually decreased, meanwhile, the total amount of matter has gradually increased by an equivalent amount. Those observations align with the predictions of the Big Bang theory, indicating that the currently dark energy should be the residual energy left over from the early Universe following the Big Bang. Because the high-energy-density cosmoses are expanding rapidly than our low-energy-density cosmos; therefore, dark matter in other cosmoses subjects to a "drag" by gravity on the stars and galaxies of our cosmos, leading to the observed accelerating expansion of the Universe.

Keywords: Dark Energy, Dark Matter, String Theory, Anthropic Principle, Multiverse.

1. INTRODUCTION

In the 1920s, Jacobus Kapteyn, the first astronomer to address the possible existence of invisible matter in the Milky Way Galaxy, used stellar velocities [Kapteyn 1922], Subsequently, some scientists: Oort (1932), Zwicky (1937), Bartusiak (1988), Stsrobinskii and Zel'dovich (1988), found unobservable matter, which was called "dark matter", amounted to more than 90 % of the mass of the entire Universe. Dark matter is real and can only be detected by its gravitational influence on visible matter. Although almost all astronomers agree on the existence of dark matter; however, after one hundred years of search, nothing has been gained.

In 1998, the High-Z Supernova Search Team published observations of type 1a supernova as standard candles [Riess et al. 1998], and in 1999, the Supernova Cosmology Project was launched [Perlmutter et al. 1999]. Two independent projects simultaneously reached the same

conclusion: a completely unexpected acceleration of the expansion of the Universe. Their discovery led to the idea of an expansion force, dubbed “dark energy”. Scientists believe that dark energy is the force that tears the Universe apart, but dark matter condenses all things, and that the interaction of these two forces forms the structure of the Universe, as we know it today.

After the Planck satellite observed the cosmic microwave background radiation, scientists deduced the cosmological parameters of Planck 2018 results VI were taken as the current situation of the Universe, that the Universe is composed of approximately 4.94% of normal matter, such as planets, stars, asteroids, and gases, etc., the remaining 95.06% is dark matter and dark energy, of which dark matter that does not radiate or absorb light accounts for approximately 26.64%, and dark energy accounts for approximately 68.42% [Aghanis et al. 2020].

Dark energy is a current scientific hypothesis, being neither matter nor radiation, its physical properties have no clue, and we do not know how it works, and dark matter is also no solution, so now all astrophysicists take them as the major difficult problems. Because the names of dark matter and dark energy come from astrophysics, we use the string theory of theoretical physics to address the major problems associated with astrophysics.

2. MULTIVERSE RESEARCH

2.1. Based on original string theory, 10-dimensional spacetime exists in the Universe.

In the 1970s, France physicist Joel Scherk and American professor John Schwarz introduced the string theory. The string theory begins with the notion that point-like particles in particle physics can also be modeled as one-dimensional objects called strings. The characteristic length scale of strings is assumed to be on the order of Planck length, or 10^{-35} meters that looks just like an ordinary particle, with its mass, charge, and other properties determined by its vibrational states in different ways.

In quantum field theory, when a string moving in the framework of time and space is so complex that three-dimensional space can no longer accommodate its motion orbit, up to nine-dimensional space must be available to meet the motion. Thus, all objects are considered a 9-dimensional space of the string. The original string theory is based on the Universe constitution of nine-dimensional space and one-dimensional time. The 10-dimensional space-time of string theory is interpreted as the product of ordinary 4-dimensional space-time and 6-extra-dimensional spaces, which have not been observed [Scherk & Schwarz 1975].

The string theory describes all fundamental forces and forms of matter and potentially provides a unified description of gravity and particle physics. Many mathematicians and physicists have attempted to break (compactify) the constitution of a ten-dimensional space-time model through spontaneous symmetry breaking, to a four-dimensional one as our known world and 6-extra-dimensional space, which is compacted to be a tiny space called Calabi-Yau

space as Planck space. Because there is no exact boundary condition to fit the real Universe and work out a theoretically solid basic geometry, no proposed method meets perfection.

Without considering compaction, the nine-dimensional space should be symmetrical, i.e., it should be symmetrical with the same weight for each dimension of space. Therefore, the Universe should still exist in an equal weight of nine-dimensional space plus one-dimensional time, so it can be argued that the string theory of the cosmic framework should still be able to maintain a complete ten-dimensional spacetime.

In multidimensional string theory, the force of gravity is the only fundamental force with effect across all dimensions. This explains the relative weakness of gravity compared to other fundamental forces (as electromagnetic force), which cannot cross into extra dimensions. In that case, dark matter could exist in extra-dimensional space, where it only interacts with matter in our space through gravity. Dark matter could aggregate in the same way as ordinary matter, forming extra-dimensional galaxies [Siegfried 1999].

Georgi Dvali and his colleagues proposed that the extra dimensions of space do not curl up into a minimum but rather are infinite in size and uncurved, just like our ordinary three-dimensional view. In character of string theory, they rethink the "extra dimensions" problem, that is, gravity can roam to any additional dimension of space. They believe that the accelerated expansion of the Universe was not caused by dark energy, but rather by gravity leaking out of our world. In particular, this theory predicts that the Universe has extra dimensions into which gravity, unlike ordinary matter, can escape. This leakage would warp the spacetime continuum and accelerate the cosmic expansion. Thus, the extra dimensions do not need to be small and compactified, but may be large extra dimensions [Dvali 2004], i.e., outside our ordinary three-dimensional space, there are the same six extra dimensions of other space usually in the Universe.

2.2. Some cosmologists accept this multiverse concept at present

In the 1950s, Hugh Everett devised “the many-worlds interpretation (MWI)” of quantum mechanics. The core of the idea was to interpret in the quantum world that an elementary particle, or a collection of such particles, can exist in a superposition of two or more possible states of being [Everett 1957].

In the 1980s, Leonard Susskind stated that it was the result of string theory, which was used as a tool or framework to describe cosmic phenomena (Susskind, 2006). MWI is a theory of multiple Universes. In this case, scientists can offer the only possible explanation: these elementary particles do not exist only in our cosmos; they may also fly around other cosmoses that are not ours. This means that there may be multiple cosmoses, called multiverse, in space, but there are only subtle differences between them, so there are still cosmoses that we do not know about.

An important aspect is to extend physical theories within a multiverse framework. The dominant expectation so far for the theory of quantum gravity (QG) has been the ‘reductionist’

hope that relies on QG producing a unique solution that resembles the general features of our Universe, but scientists have failed. The three different and important theories: quantum mechanics, string theory, and inflation, predict the existence of the multiverse, which scientists believe is hardly co-incidental. The existence of the multiverse can be expected from the underlying fundamental theory.

David Deutsch is a leading figure in multiverse theoretical physics. He believes that this multiverse theory is the only explanation for the strange phenomenon in quantum mechanics because it is based on rigorous mathematical equations and many experimental results [Deutsch 2010]. Although more than 50 years have elapsed since the first discussion of the “many worlds” by Everett, there is not any new step to set the foundations and the ontology of the multiverse and of this new field in physics.

2.3. The fluctuation map of microwave background radiation may provide hard evidence of another cosmos

In June 2001, NASA launched WMAP, which was designed to detect residual cosmic radiation heat in the Universe after the Big Bang and drew a full fluctuation map of microwave background radiation throughout the Universe. In 2009, the European Space Agency’s partnership with NASA launched the Plank Satellite, which can detect tiny temperature fluctuations in this radiation. Then, a fluctuation map of cosmic microwave background radiation was drawn with greater accuracy.

In general, scientists tend to think that the radiation is evenly distributed, but the full map shows a different fact: there is a powerful center in the sky in the southern half of the map and a seemingly hole-like "cold spot" that cannot be explained by existing physics knowledge, where galaxies are accelerating away [Rudnick et al. 2007].

From this anomaly, some scientists have proposed multiverse perspectives to explain the cold spot. Scientist have predicted that string theory does not predict a unique Universe; on the contrary, it predicts a multiverse (Mersini-Houghton, 2008). In 2005, scientists predicted that anomalies in radiation existed that could only have been caused by gravitational pulling on our cosmos from others as it formed during the Big Bang [Woit 2013]. The "cold spot" in the southern half of the fluctuation map of the Universe may be the first "hard evidence" of another cosmos than ours that exist has been found by scientists [Leake 2013].

3. THEORIES AND METHODS

3.1. The Universe should be a 3-cosmic framework from Causality and Anthropic Principles

Without compacting the nine-dimensional space of the Universe, the ten-dimensional spacetime of string theory is considered to exist universally. According to “Causality”, an effect cannot occur before its cause, which means that time has one direction and cannot be divided into different parts. Thus, one-dimensional time is taken as the common standard for the order of events in the Universe.

According to “Anthropic Principle”, which is the simple fact that we live in a Universe set up to allow for our existence. This means that 3-dimensional space and 1-dimensional time, called 4-dimensional spacetime, are taken together as one cosmos as our living world. Therefore, the 9-dimensional space can be divided into three portions, each with a common standard time. It means that there is a 3-cosmic framework in the Universe, called triple cosmoses, i.e., the Universe contains three cosmoses located in the same nine-dimensional space of the Universe.

According to string theory, a 3-cosmic framework of the Universe in which our cosmos describes the world of general matter as we know it, while others describe another world, which we know nothing. Among any other cosmoses, there are no fundamental forces of nature except gravity; in other words, the graviton in the field of gravity can penetrate all three cosmoses; however, light (electromagnetic wave) cannot that means among the cosmoses cannot be observed directly with each other.

According to this 3-cosmic framework of the Universe, there are triple cosmoses in the whole space, namely 1st cosmos, 2nd cosmos and 3rd cosmos, where U1, U2, and U3 are used instead. There are 4 fundament forces (including gravitational force, strong nuclear force, weak nuclear force and electromagnetic force) exist in the Universe. According to the string theory, in the 3-cosmic framework of the Universe there is no force between any two cosmoses except gravitational force, i.e., cosmoses cannot directly interact with each other, which is the characteristic of dark matter. Therefore, dark matter will not be observed, but it should exist in cosmoses other than ours.

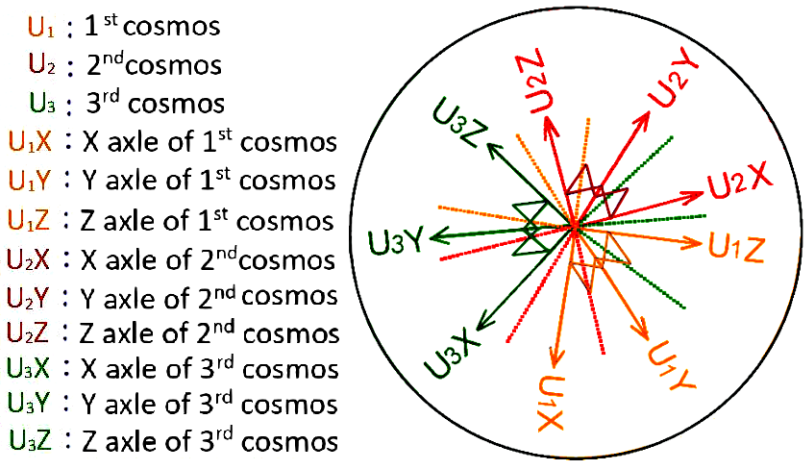

Figure1. The imitation Schematic diagram of nine-dimensional space in the 3-cosmic framework of the Universe.

As the figure 1, all the 3 cosmoses (U1, U2, and U3) exist, but none of the fundamental forces can affect each other except gravity; for example, if U1 is our cosmos, we cannot observe U2 and U3. The 3 axles (X, Y, and Z) all perpendicular to each other in each cosmos. In the diagram, assuming a star P appears in our cosmos, which has 9 coordinates: U1Xp, U1Yp, U1Zp, U2Xp, U2Yp, U2Zp, U3Xp, U3Yp, and U3Zp in the Universe, because the other

cosmoses cannot observe the star P, its coordinates are only denoted by Xp, Yp and Zp [Ho 2022].

3.2 Exploring dark matter starts from the interior of the Earth

Based on original string theory and the 3-cosmic framework of the Universe, we can investigate dark matter in cosmoses other than our own. The best method for exploring dark matter is to start from Earth, where we live. In the current Earth model utilized in seismological investigations, such as body-wave travel times, surface-wave dispersion, and free oscillation periods for researching the chemical composition and density distribution of the Earth, the portions of the crust and the upper mantle have been analyzed with satisfactory accuracy. However, regarding the lower mantle and core, a number of questions remain to be answered.

About the Earth's interior, the constitution of the deep interior is uncertain with some difficulties. In order to conduct further investigation, the Preliminary Reference Earth Model (PREM) [Dziewonski & Anderson 1981] is taken as the normal Earth model in this paper. At the core-mantle boundary (CMB) of this model, the solid portion of the lowermost mantle has a density of 5.56645 g/cm^3, which jumps to 9.90349 g/cm^3 in the liquid portion of the top core, a density jump of 77.91%, so the CMB is also called "Gutenberg discontinuity". In the current field of geosciences, the results are taken for granted. However, in the PREM the density jumps significantly at the CMB, all investigations cannot confirm the data directly, so, research about the interior constitution of the Earth is needed, especially at the CMB.

It has been well known that there are two convections circulating individually below the crust to the lower mantle and in the outer core itself. The mantle and core are not in chemical equilibrium, and the fine structure of the CMB is not well understood. Although some hypotheses such as the existence of a D" layer in the lower mantle and iron combined with oxygen as the primary alloying constituent of the outer core have been suggested, and a lot of advances in this research have come out, there are also some discrepancies in the interior of the Earth [Creager & Jorden 1986].

3.3 Arguments at core-mantle boundary

To investigate the outer core, a different view of the deep interior of the Earth should be taken to analyze the Earth's constitution, composition, temperature, and pressure from a different perspective of the core, special arguments are proposed. With regard to the Earth's interior, the constitution of the deep interior is uncertain with some difficulties and considering some different conclusions of many experts' studies over the years, we may get another perspective. There are some arguments in the topic of the CMB as in the following.

1. Ramsey (1948) and Lyttleton (1973) challenged the concept of an iron core, stating that the CMB is the boundary of Ramsey's phase-change, not silicates and iron core interface.

2. Knopoff (1965) showed that the bulk modulus remains constant so that the density distribution should be continuous at the CMB.

3. Buchbinder (1968) studied the variation in the reflection amplitudes of seismic waves and found that they showed a phase-change at the CMB.

From items 1, 2, and 3 above, it can be initially identified that the materials of mantle and core mix with each other, and the density distribution between the lower mantle and the outer core should be consistent to solve some geophysics problems. The main components of the outer core should be considered as the same ingredients of molten rock and/or mineral silicates, which are chemically consistent with the ingredients found the lowermost mantle.

The isotopic composition of lavas associated with mantle plumes has previously been interpreted in the light of core–mantle interaction, suggesting that mantle plumes may transport core material to Earth's surface [Mundl-Petermeier et al. 2020; Rizo et al. 2019; Horton et al. 2023; Mundl et al. 2017]. The combined ruthenium and wolfram isotope systematics of Hawaiian basalts are best explained by simple core entrainment and addition of core-derived oxide minerals at the CMB [Messling et al. 2025]. The main composition of the outer core should be considered as the same ingredients of molten rock and/or mineral silicates, which are chemically consistent with the lowermost mantle and from the core brings some matter, such as the metal platinum [Hecht 1995], osmium-187 [Walker et al. 1995] have come all the way to the surface of the Earth that flows between the F layer and the Earth's crust, causing the more than 10 km relief of the CMB [Morelli & Dziewonski 1987].

3. 4 The topography of the CMB revealed that both sides were made of the same materials

A sufficient quantity of high-quality digital data from two global networks: a network for very long-term seismology [Agnew et al. 1976] and a seismic research observatory [Peterson et al. 1976], which began operation in the mid-1970s and developed over four decades, provided the framework of formal analysis. The availability of computers made the handling of immense amounts of data feasible and the large-scale calculations necessary for three-dimensional problems. Geophysicists recorded on the Earth more than 15,000 times magnitude 4.5th-class earthquake data, input a seismic laboratory computer, drawn a three-dimensional topographical interior map of the Earth, and produced computer tomography X-ray photographs, producing the CMB topography, which is found in boundary of solid mantle and liquid outer core. Maps of the CMB topography have been derived on the basis of seismological inversions of long-wave travel times to construct three-dimensional maps with the magnitude of amplitudes from ±3 km up to ±6 km (largest relief 12 km) and with 3000～6000 km scale lengths [Doornbos & Hilton 1989; Forte & Peltier 1991; Neuberg & Wahr 1991; Rodgers & Wahr 1993; Obayashi & Fukao 1997; Boschi & Dziewonski 1999, 2000; Garcia & Souriau 2000; Sze & van der Hilst 2003; Yoshida 2008; Soldati et al. 2013; Soldati et al. 2014].

In three-dimensional maps of the Earth's interior, the topography of the CMB differs from that predicted by hydrostatic equilibrium theory, which contains information important to geodynamic processes and geomagnetic secular variation. The topography of the CMB is likely due to convection in the overlying mantle [Young & Lay 1987]. Ruff and Anderson (1980)

argued for dynamo action in the core maintained by differential heating of the core by the mantle, and some agreements with them were probably determined by processes in the core [Bloxham & Jackson 1990]. The depressed regions of the topography are dynamically supported by down welling of cool mantle material [Lay 1989], indicating that the relief is dynamically supported and provides coupling between the solid mantle and the fluid core. Scientists suggest further effects due to topography associated with subduction slabs, which may have a mechanical rather than thermal effect on the flow [Gubbins & Richards 1986].

It is obvious in terms of geodynamic processes that only the vertical interactions of the material and the temperature between the lowermost mantle and the outer core are the main causes. In order to maintain the about 10 km of relief, the density difference between the liquid and solid states at the CMB must be very small; so, the density of the materials between both sides at the CMB must be similar or equal, i.e., the hypothesis that the same materials between the solid mantle and liquid core change state with each other at the CMB.

3.5 Examining the chemical composition of the core

In order to confirm the favorable constitution of the Earth, the chemical composition of its core must be further investigated. The composition of the Earth's core is one of the most important and elusive mysteries in geophysics. There is no perfect explanation for the chemical equilibrium between the core and the mantle, and the inner core is not in thermodynamic equilibrium with the outer core [Jeanloz 1990].

The physical and chemical properties of the lower mantle are poorly understood, and the understanding of the coupling mechanisms between the mantle and the core is poor at all timescales. However, the CMB sets boundary conditions for processes occurring within the core, a well-known fact. The topography and lateral temperature variations in the lowermost mantle may have an indistinguishable effect on the magnetic field [Bloxham & Gubbins 1987]. Secular variations with periods shorter than a million years but longer than several years almost certainly originate from processes operating in the outer core; unfortunately, there is not yet consensus as to what those processes are [McFadden & Merrill 1995].

In three-dimensional maps, topographic models represent instantaneous, low-resolution images of a convicting system. Detailed knowledge of mineral and rock properties that are poorly understood at presents required. A complex set of constraints on the possible modes of convection in the Earth's interior that have not yet been worked out; this will require numerical modeling of convection in three dimensions. Thus, the interpretation of the geographical information from seismology data in terms of geodynamic processes is a matter of considerable complexity. The topography of the CMB can be sustained only by dynamic processes, and these processes must be critically understood [Woodhouse & Dziewonski 1989].

The fine structure of the CMB is not well known, but it contains information that is important to geodynamic processes in the mantle, or the magnetic fields generated in the outer core [Anzellini et al. 2013]. As stated previously, the main components of the outer core were

similar to those of the lower mantle, i.e., mineral silicates. Based on mineralogy, the main mineral of the mantle is pyrolite, a silicate-containing compound, and the main components of the outer core are also pyrolite but only in liquid form. Under the same conditions, the higher the temperature at which common minerals are produced, the lower is the polymerization rate, and vice versa. The closer the crystal minerals of the mantle were exposed to temperature and pressure, the more the polymerization losses of the crystalline minerals. The bonding forces of the mineral compounds are then destroyed, and crystallization gradually diminishes.

In the F-layer of the deeper core, the high temperature more than 6000°C [Condie 1997], polymerization may cease completely, and the bonding power of ions mostly loses, and only the electronic bonding force exists. All the ions and molecules may become unbounded. Therefore, the molten rock or magma becomes a mixture of oxides such as FeO, MgO, NiO, SiO_2, Fe_2O_3, Al_2O_3, Cr_2O_3, etc., and metals such as Fe, Ni, and Mn.

According to the temperature profile of the Earth's interior, the center of Earth is made of high-temperature material, which is the hottest point, estimated to be 7000°C [Kubala & Mahan 1996], which is hotter than the surface of the Sun. In the F-layer, the chemical components may reduce the viscosity; the full fluid oxides and metals can flow, diffuse, float, or sink more freely according to their specific gravity. Estimation of Fe melting temperature at the ICB pressure based on static compression data spans the range 6230 ± 500°K [Anzellini et al. 2013].The F-layer above the ICB, in which Fe likes snowflakes falling in the inner core [Gubbins, Masters & Nimmo 2008].

There is a large amount of iron oxides (FeO, Fe_2O_3) in the mantle, and the deeper the mantle, the higher the proportion of iron oxides. An iron oxide with a metal-like density and electrical properties at high pressure and temperature exists in the Earth's core and may be a compromise between extreme views of the metallic phase and inconformity with the high cosmic abundance of oxygen [Altshuler & Sharipdzhanov 1971]. From this information, the outer core is rich in iron oxides are proposed.

In view of the topography, the downward migrating magma rich in iron oxides was affected by diffusion, obstruction of the inner core, tangential geostrophic flow, and toroidal flow. Thus, the fluid flowed westward, which may have caused geomagnetic secular variation. Under low viscosity, the oxides and metals can flow easily vertically and horizontally, allowing mutual oxidation-reduction reactions to take place in the F-layer. The active light metals take oxygen from the heavy metal oxides and are further oxidized into light metal oxides, whereas the heavy metal oxides are reduced to heavy metals and precipitate in the inner core. For example:

$Ca + FeO \longrightarrow CaO + Fe \downarrow$

$3Mg + Fe_2O_3 \longrightarrow 3MgO + 2Fe\downarrow$

$2Al + Fe_2O_3 \longrightarrow Al_2O_3 + 2Fe \downarrow$

$2Cr + 3FeO \longrightarrow Cr_2O_3 + 3Fe \downarrow$

$Mn + NiO \longrightarrow MnO + Ni \downarrow$

CaO, MgO, Al_2O_3, Cr_2O_3, and MnO float in the F-layer, and Fe_2O_3, FeO, and NiO become Fe and Ni, respectively, sinking down to be the main components of the inner core. These oxidation-reduction reactions are exothermic processes that produce large amounts of heat. Reduced iron alloys with certain amounts of Ni settle at the ICB. By far the most provocative mechanism, the F-layer should be maintained through the interaction of the separated melting and solidifying regions distributed over the ICB [Alboussière, Deguen & Melzani 2010].

In the primordial planet, there were substantial quantities of uranium and thorium sunk to the Earth's core, and some evidence is presented for the existence of it [Herndon 1993]. In August 2002, Oak Ridge Lab of United States Federal Energy in National Geographic Society report a new achievement in scientific research that 6371 km below the surface of the Earth's center has a diameter of 8 km, consisting of uranium and plutonium fast breed natural fission reactors, which can generate new fuel on its own and are a source of energy needed for all life on the Earth. In the F-layer, magma diffuses and absorbs a large amount of heat to rise to the CMB, where it condenses into solid rock as the beginning of the process of a large convection cell starts anew.

The great amount of heat produced from radioactive elements generated nuclear energy, chemical reaction heat in the F-layer, and nuclear fission heat near the center of the Earth became the power sources for the geo-dynamo of great convection cells, which are the flows of the magma and the solid rock migrating up to the crust and down across the CMB to the F-layer [Ho 2019] as the figure 2. Therefore, a new Earth model is established.

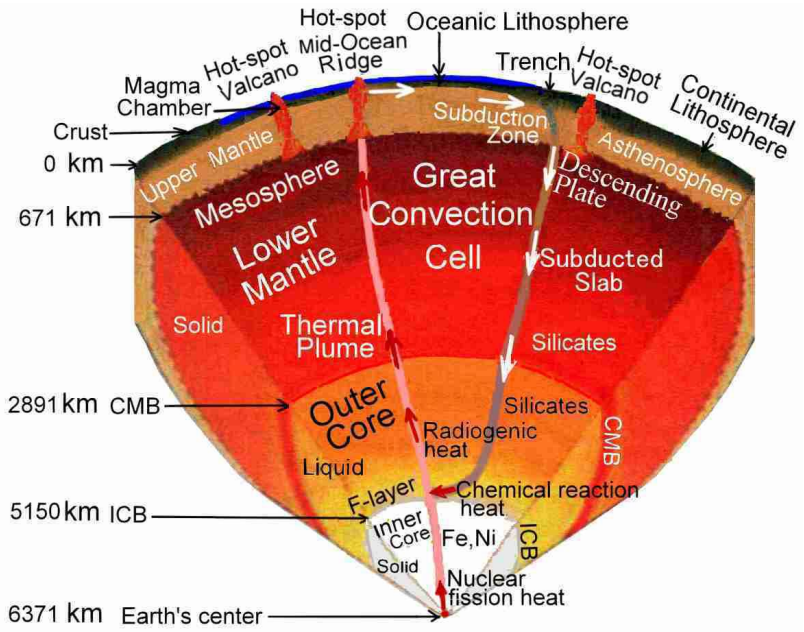

Figure 2. A Schematic diagram of the great convection cell, heat flow, and the composition of Earth's interior.

4. MATHEMATICAL FORMULATION

4.1 Digital evaluation of data in new Earth model

Based on the new conception, we apply a simplified method to evaluate the Earth's mass and moment of inertia. To calculate the Earth's data, the density distribution follows the divisions of the PREM into 94 levels, including 82 thin shells. The thickness of each shell is not greater than 100 km and so small compared with the Earth's radius of 6371 km that the density is linear variation within it. Then, a simplified method is applied to calculate the information of the Earth in order to simplify the calculation. The formula for the mass M of a uniform sphere can be derived as $M = (4/3)\pi\rho R^3$. The mass ΔM of each shell in the Earth's interior can be calculated as

$$\Delta M = (4/3)\pi\rho_t R_t^3 - (4/3)\pi\rho_b R_b^3 \quad (1)$$

Where: ρ_t, ρ_b are the densities at the top and bottom, respectively, of a single shell, and R_t and R_b are the radii of the top and bottom in a shell. Because the difference between R_t and R_b is small and the density is regarded as linear variation in the shell, the mean value $\overline{\rho}$ of both ρ_t and ρ_b is substituted for ρ_t and ρ_b in order to simplify the calculation. Then equation (1) becomes

$$\Delta M = (4/3)\pi\overline{\rho}(R_t^3 - R_b^3) \quad (2)$$

The moment of inertia ΔI of each shell in the Earth's interior can be calculated as

$$\Delta I = (8/15)\pi\overline{\rho}(R_t^5 - R_b^5) \quad (3)$$

From fluid mechanics, in a region of uniform composition, which is in a state of hydrostatic stress, the gradient of hydrostatic pressure can be expressed as

$$dP/dR = -g\rho \quad (4)$$

Here, P and R are the pressure and radius, respectively, in the region; ρ is the density at that depth; g is the acceleration due to gravity at the same depth. If the effect of Earth's rotation is negligible, the potential theory shows that g is resulted only from the attraction of mass M within the sphere of radius R through

$$g = GM/R^2 \quad (5)$$

Where: G is the gravitational constant ($6.6726\times10^{-11} m^3/kg.s^2$). Equation (5) substitutes into equation (4) and integrates it. In order to simplify the calculation, ρ and M are substituted by $\overline{\rho}$ and $\overline{m}$, which are considered constants in the thin shell and are irrelative to P and R. The result becomes

$$\Delta P = (1/R_b - 1/R_t)G\overline{m}\overline{\rho} \quad (6)$$

Where: ΔP is the difference in pressure between the top and the bottom in a layer of the Earth, and $\overline{m}$ is the mass of a sphere as the mean value of the masses of the sphere within the

top radius R_t and the bottom radius R_b, respectively, of a shell. Equation (6) cannot be applied to the center of the Earth, where is a discontinuous point. To integrate the portion of the center, the other form is applied as follows:

$$\Delta P_c = (2/3)\pi G\bar{\rho}^2 R_c^2 \qquad (7)$$

Where: ΔP_c is the difference in pressure between the radius R_c and the center of the Earth at the center. The acceleration due to gravity g of each layer can be derived from equation (5). According to the observation data, the moment of inertia for the polar axis of the earth is $0.3309 M_e R_e^2$ and about an equatorial axis is $0.3298 M_e R_e^2$ [Garland 1979]. The Earth is regarded as a sphere, of which the moment of inertia is determined to be 80286.4×10^{40} g.cm^2 by taking the mean value of both figures, where M_e is the Earth's mass of 5974.2×10^{24} g and R_e is the equatorial radius of 6378.14 km.

To examine the accuracy of the applied equations in the simple method, we applied the density distribution of the PREM to calculate the Earth's mass, moment of inertia, pressure, and acceleration due to gravity, and is shown in Table 1 (http://newidea.org.tw/pdf/S60.pdf). The deviation of calculated Earth's pressure between the PREM and the simplified method are listed in Table 2 (http://newidea.org.tw/pdf/S61.pdf) and shown the curves of pressure P and deviation E of the PREM in the Figure 3.

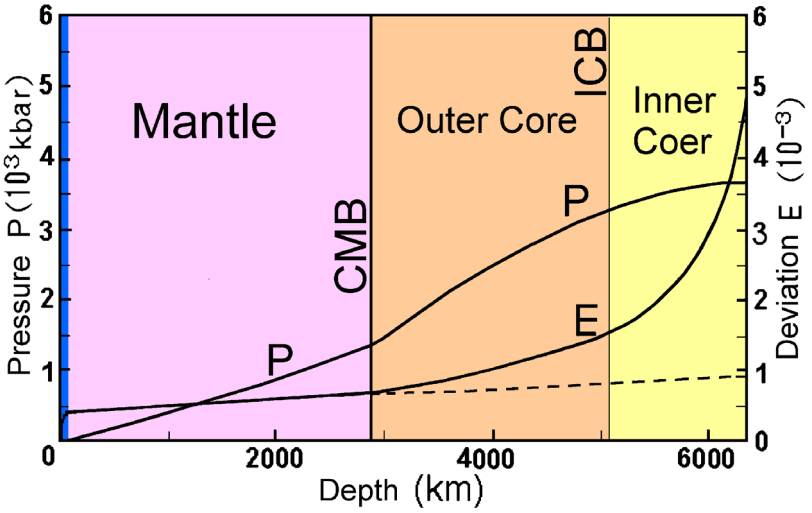

Figure 3. Pressure P of the PREM and deviation E of the calculated pressure using the simplified method from the value of P

The calculated data of the simplified method from the density distribution of the PREM as compared with the data of the observed data of the Earth are listed in Table 3 [Ho 1993].

Table 3. The calculated data of the simple method from the density distribution of the PREM as compared with the data of the prem and the observed data of the Earth

Data of the Earth	Mass	Moment of inertia	Pressure at the CMB	Pressure at Earth's center	Gravity at the CMB	Gravity at Earth's surface
Unit	10^{24} g	10^{40}g.cm^2	K bar	K bar	cm/sec^2	cm/sec^2

PREM and observed data	5974.200	80286.400	1357.509	3638.524	1068.230	981.560
Calculated values	5973.289	80205.664	1358.335	3655.973	1068.680	981.959
Deviation %	-0.0152	-0.1006	+0.0608	+0.4796	+0.0421	+0.0406

From Table 3 the deviations of the calculated Earth's values from the PREM data and the observed Earth are nearly within 0.1%, except for the pressure at the Earth's center. This indicates that the calculated values are very close to the current data and that the simplified method is acceptable and useful.

The calculated pressure of 3655.973 kbar at the Earth's center is higher than the PREM data of 3638.524 kbar by 0.4796 %, about 8 times of deviation E at the CMB. From the figure 4, the deviation E of the pressure curve from the crust to the CMB is nearly a straight line, indicating that the calculated pressures have systematic errors from the error theory; however, from the CMB to the Earth's center, the slope of curve E increases sharply above the dashed line, which is the straight line extended from the CMB. This indicates that there is considerable discrepancy in the core. We may suppose that the structure of the PREM core, which greatly affects its core pressure, is something wrong that shows PREM in the Earth's core section need to be explored in more detail.

4.2 four curves of density distribution are proposed to match the known conditions

As stated previously, the difference in density between the outer and inner cores must be substantial. Jeanloz and Ahrens (1980) conducted shock wave experiments, in which they found that the density of FeO was 10.14 g/cm^3 when reduced to the core temperature and 250 GPA pressure, and under the same conditions, the density of Fe was 12.62 g/cm^3 [McQueen et al. 1970] when FeO became Fe. The difference between the two is 2.48 g/cm^3, which is higher than all other evaluated values.

From this information other than the PREM, the density jump between the lighter liquid outer core and the solid inner core seems to be too large to represent a simple volume change during condensing as the same major components change from a liquid state Fe to a solid-state Fe. The composition of the outer core is not likely to be the same as that of the inner core because a liquid in equilibrium with a solid phase in a multi-component system does not have the same composition as a solid [Hall & Murthy 1972]. We inferred that the major component of the outer core was mineral silicates, but iron was present in the solid inner core.

In order to investigate the structure of the Earth, particularly the core, four curves of density distribution are proposed to match the known conditions. From the crust to the CMB the curves of density distribution are adopted as the PREM, and from the CMB to the ICB, four different plotted curves were assumed. Due to a small jump in the P-wave velocity at the boundary of the F-layer in the outer core, the slope of the density curve was nearly as steep as that of the PREM. There is a discontinuity of P-wave velocity at the ICB, on the basis of the free oscillation periods, Derr (1969) inferred an Earth model DI-11 by least-squares inversion

with an average shear velocity of 2.18 km/sec in the inner core and a jump in density of 2.0 g/cm^3 at its boundary that satisfied the known mass and moment of inertia, so, a density jump of Derr's suggestion (2.0 g/cm3) is used. In the inner core, the slope of new density curve and PREM's was the same. The four density curves of the assumed Earth model compared with the PREM are shown in Figure 4.

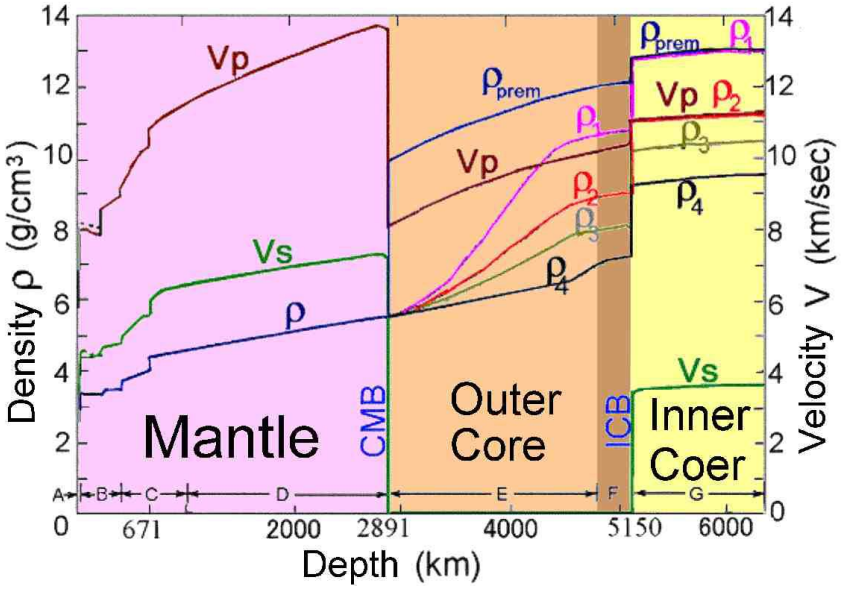

Figure 4. These densities ρ of the new Earth models 1, 2, 3, and 4 were compared with the PREM's.

From equations (2) and (3), the mass and the moment of inertia of the four new Earth model can be determined and compared with the current measured data of the Earth's mass of 5974.2×10^{24}g and moment of inertia of 80286.4×10^{40} g.cm^2 (1990s), so the differences are found to be very large, as shown in Table 4.

Table 4. Insufficiencies of mass and moment of inertia in the four new Earth models

Earth's Data	Unit	Observed value	New Model 1.	New Model 2:	New Model 3.	New Model 4:
Mass	10^{24}g	5974.200	5409.024	5268.126	5204.761	5121.820
Insufficiency	10^{24}g	-	565.176	706.074	769.439	852.380
Moment of inertia	10^{40}g.cm^2	80286.400	77007.472	76571.028	76378.768	76126.841
Insufficiency	-	-	3278.928	3715.372	3907.632	4159.559

The insufficiency in the Earth's mass and moment of inertia, called the missing mass and moment of inertia, are relative to the gravity of dark matter in astrophysics. It can only be obtained by comparing the observed data of the Earth, which cannot be detected directly and answered clearly through ordinary Earth sciences. To solve the problems of insufficiencies, a new study of the Earth is attempted by using contemporary physics. If we can successfully explain that the insufficiencies exist in a suitable condition, such as the missing mass and moment of inertia are a dark planet inside the Earth, a new Earth model will be established.

4.3 Evaluating the data of the dark planet in a new Earth model

Proceeding with this assumption, the missing mass and moment of inertia of the Earth are assumed to be those of cold dark matter (CDM), which may constitute a normal planet. In order to find a solution for this paper, dark matter is compared to Mars. The average radius of Mars is 3397 km, and the mass 642.40×10^{24} g. Kaula and his colleagues studied the moment of inertia of Mars and obtained the maximum allowable mean value is 0.3650 MR^2, i.e., 2689.8×10^{40} g.cm^2 [Kaula, Sleep & Phillips 1989]. The insufficient data of 4 new Earth models roughly approach to the Mars‟, So, the dark matter is considered as a planet, called a dark planet, whose form is similar to Mars, and whose characteristics are based on the inner planets of the solar system. To cut a figure of the dark planet, it is considered a sphere whose radius and density can be calculated from the insufficiencies in the Earth's mass and moment of inertia through the simplified method. The dark planet data can be calculated as following.

Considering the density of rock on the surfaces of the Earth and Moon, a surface density of 2.70 g/cm^{3}of the dark planet is proposed. Under the condition that the density of a layer is proportional to its depth, a trial value of density at the center of the dark planet is selected. Applying equations (2) and (3) to calculate the mass and moment of inertia of each shell, the total mass and moment of inertia of each shell can be obtained. Because the radius and center density of the dark planet are hypothetical values, the total mass and moment of inertia must correspond to the insufficiencies of the Earth's mass; therefore, it is necessary to use a trial-and-error approach to determine the proper radius and center density.

Since the Earth's orbit around the Sun may be affected by the gravity of the dark planet, no abnormal effects on the Earth have been observed. It is assumed that the gravity centers of the Earth and the dark planet coincide at the same time. It is inferred from the phenomenon in which the same side of the Moon always faces the Earth, meaning that the Earth and the dark planet may rotate synchronously.

Assuming that the gravity centers of the Earth and the dark planet coincide at a single point, and both rotate synchronously, the total mass and moment of inertia may be obtained from. Based on mechanics, the gravity of each shell inside the Earth is affected by the mass of the Earth and the dark planet within its radius. The pressure difference $\Delta P'$ between the top and bottom of a shell in the Earth is calculated through

$$\Delta P' = (1/R_b - 1/R_t)G\overline{M}'\overline{\rho} \qquad (8)$$

Where: $\overline{M}'$ is the mean value of the total mass of the Earth and the dark planet within radius R_t and R_b. Equation (8) cannot be applied to the Earth's center. The average density $\overline{\rho}'$ of the central portion combined with the Earth and the dark planet within radius R_c can be calculated as follows:

$$\overline{\rho}' = (M_c + M_d) / [(4/3)\pi R_c^3] \qquad (9)$$

Where: M_c and M_d are the masses of the central portion on the Earth and the dark planet, respectively. The difference in pressure $\Delta P_c'$ between the top and center of the central portion of the Earth can be obtained as

$$\Delta P_c' = (2/3)\pi G \overline{\rho}\,\overline{\rho}' R_c^2 \quad (10)$$

Based on the characteristics of the inner planets of the solar system except for Mercury, a planet with a larger radius has a higher average density. Therefore, the radius and average density of a suitable dark planet must be compatible with the characteristics of the inner planet in the solar system. The data of the four new Earth models and each dark planet were compared with the data of the current Earth and the PREM (Table 5).

Table 5: Calculated data of the four new Earth models compared with the data of the current Earth and the PREM

Kind of Earth's model	The Earth planet							The dark planet					Suitability
	Radius	Average density	Mass	Moment of inertia	Center density	Center pressure	Coefficient	Radius	Average density	Mass	Moment of inertia	Coefficient	
Unit	km	g/cm^3	10^{24} g	10^{40} g.cm^2	g/cm^3	kbar	C	km	g/cm^3	10^{24} g	10^{40} g.cm^2	C	
PREM	6371	5.5150	5974.200	80286.400	13.08848	3638.524	0.3309						
Model 1	6371	4.9945	5409.024	77007.472	13.08848	3283.754	0.3508	3808.414	2.4427	565.176	3278.928	0.4000	no
Model 2	6371	4.8635	5268.126	76571.028	11.29785	3039.584	0.3581	3732.304	3.2421	706.074	3715.372	0.3777	no
Model 3	6371	4.8050	5204.761	76378.768	10.46002	2934.587	0.3615	3717.755	3.5747	769.439	3907.632	0.3674	no
Model 4	6371	4.7284	5121.820	76126.841	9.49821	2805.297	0.3662	3700.375	4.0161	852.380	4159.559	0.3564	good

The average radius and average density of Mars are 3397 km, 642.40×10^{24}g respectively. In the table 5, the new Earth model 4, the values of the radius and the average density of the dark planet are 3700.375 km and 4.0161 g/cm^3, which are larger than those of Mars, and the coefficient 0.3564 is more suitable; therefore, this model is found to be the more suitable one.

The precise data for the Earth and the dark planet were calculated from the density distribution of the new Earth model 4. The data for the Earth planet are listed in Tables 6 (http://newidea.org.tw/pdf/S62.pdf), the dark planet is listed in Table 7 (http://newidea.org.tw/pdf/S63.pdf), and the global data for the new Earth model in Table 8 (http://newidea.org.tw/pdf/S64.pdf). After the calculation, the new Earth model compared with those data of the current Earth and the PREM are listed in Table 9.

Table 9. The calculated data of the new Earth model compared with those of the Earth and the PREM

Data of planet	Radius	Mass	moment of Inertia	Average density	Center density	Center pressure	Coef-ficient
Unit	km	10^{24}g	10^{40} g.cm^2	g/cm^3	g/cm^3	kbar	C
PREM and observed Earth	6371.000	5974.200	80286.400	5.515	13.08848	3638.524	0.3309
Earth planet	6371.000	5121.820	76126.841	4.7284	9.49821	2805.297	0.3662

Dark planet	3700.375	852.380	4159.559	4.0161	7.96097	1115.272	0.3564

Finally, a planet of dark matter with a radius of 3700.375 km, approximately 1.33 times that of Mars, exists reasonably inside the Earth but in other space than ours. The dark planet inside the Earth should be confirmed by Chandler wobble [Ho 2024].

The calculated density of the Earth's center was 9.49821 g/cm^3, which is much lower than the density of 13.08848 g/cm^3 of the PREM. The pressure was 2805.297 kbar, which is much lower than the 3638.524 kbar of the PREM. The composition of the inner core is generally believed to be predominantly Fe with a small amount of alloyed Ni. From the pressure-density Hugoniot data, the density of iron under 2805.297 kbar of pressure is about 12.7 g/cm^3 [Ahrens 1980], which is much greater than that of the new Earth model by 25%. The inner core is not pure iron but contains a significant fraction of light components [Ringwood 1984; Jephcoat & Olson 1987], which explains why the density of the inner core is much smaller than the current value. Therefore, an inference that the composition of the inner core is predominantly Fe, alloyed with a small amount of Ni, and combined with a significant number of oxides is suggested.

4.4 Dark planet should be recognized inside the Earth from Chandler wobble

It is difficult to directly examine the existence of dark matter; however, this should be recognized from Chandler wobble. Referring to the orientation of the rotation axis of the Earth in space in addition to both precession and nutation, there is a wobble on the instantaneous axis of rotation of the Earth. The wobble alters the position of a point on the Earth relative to the pole of rotation. In the 1890s, Chandler pointed out that there are two distinct kinds of the wobble periods. The first is a period of 12 months, and the second is a period of 433 days, which is approximately 14 months [Chandler 1891]. The former, called annual wobble, is obviously affected by the seasonal climate. The latter, called Chandler wobble, has not been solved for more than one hundred years. The Chandler wobble is a small deviation that changes by approximately nine meters at the point on the surface of the Earth’s rotation axis.

Gross (2000) found that two-thirds of the Chandler wobble was caused by fluctuating pressure on the seabed, which, in turn, is caused by changes in the circulation of the oceans caused by variations in temperature, salinity, and wind. The remaining third is due to atmospheric fluctuations. The full explanation of this period also involves the fluid nature of the Earth’s core and oceans. The wobble, in fact, produces a negligible ocean tide with an amplitude of approximately 6 mm, called a "pole tide", which is the only tide not caused by an extraterrestrial body. While it has to be maintained by changes in the mass distribution or angular momentum of the Earth's outer core, atmosphere, oceans, or crust (from earthquakes),

for a long time the actual source was unclear, since no available motions seemed to be coherent with what was driving the wobble.

It is inferred from the phenomenon, in which the same side of the Moon always faces the Earth, meaning that the Moon and the Earth rotate synchronously. The same phenomenon will happen to the Earth and the dark planet in which both rotate synchronously, but the rotation axes of both are impossible to coincide with each other, i.e., an angle between the two rotation axes produces the Chandler wobble as the precession and nutation due to the effects of the Sun and Moon on non-parallel rotation axes with the Earth's. Therefore, the effect of Chandler wobble should confirm the existence of a dark planet inside the Earth but in another cosmos than ours [Ho 2019].

5. THE EXPLORATION OF DARK ENERGY

5.1 Dark energy should be the residual energy of the Universe after the Big Bang

Dark energy is one of the most mysterious phenomena in current physics, and we used "The Big Bang Theory" to exploring it. Lemaître (1927) proposed "The Big Bang Theory". He described that at the beginning of the Big Bang, the Universe was made up of high-temperature and hot energy with uniformity and isotropy, but no matter. When this hot energy expands rapidly outward, an exponential inflation occurs [Guth 1982]. As the Universe expands rapidly and temperature decreases, the distribution of energy changes slightly, according to the famous equation of Einstein ($E=MC^2$) for gradual energy and mass interchange, creating the earliest substances.

In 1964, the discovery of cosmic microwave background radiation by radio astronomers Penzias and Wilson was the most important evidence to test the Big Bang Theory [Penzias & Wilson 1965]. Then more and more astronomical and physical evidence came out, such as Cosmic Background Explorer (COBE) [Bennet 1993], WMAP and Planck Satellite, when their detected spectrum was measured to map its black body radiation curve, the Big Bang Theory became more complete, and scientists believed in it.

In 2018, the Plank satellite detected tiny temperature fluctuations in the radiation of the Universe. These fluctuations reflect the baryon density of the Universe before galaxies formed. Normal matter (baryon) density Ω_b from galaxies and stars accounts for only 4.94 % of the Universe's composition, with the rest missing substance, including dark matter density Ω_c, which accounts for 26.64 %, and mysterious dark energy density Ω_Λ, which accounts for 68.42% [Aghanim et al. 2020].

To research dark energy, we applied a table of cosmological parameters from 1-year WMAP results to Planck 2018 results, which were selected one set at each detection under the condition that kept Hubble constants nearly gradually decrease and are shown in table 10.

Table 10. The cosmological parameters obtained from the data of WMAP and Planck satellite

Source / Symbol	1-year WMAP [Spergel et al., 2003]	3-year WMAP [Spergel et al., 2007]	5-year WMAP [Komatsu et al., 2009]	7-year WMAP [Komatsu et al., 2011]	9-year WMAP [Bennett et al., 2013]	Planck 2013 [Ade et al., 2014]	Planck 2015 [Ade et al., 2016]	Planck 2018 [Aghanim et al., 2020]
H_o	71.0	70.4	70.5	70.2	70.0	68.14	67.31	67.32
Ω_Λ	73.22%	73.2%	72.6%	72.5%	72.1%	69.64%	68.5%	68.42%
Ω_m	26.78%	26.8%	27.32%	27.43%	27.9%	30.36%	31.5%	31.58%
Ω_b	4.44%	4.41%	4.56%	4.58%	4.63%	4.79%	4.9%	4.94%
Ω_c	22.34%	22.39%	22.8%	22.9%	23.3%	25.43%	26.42%	26.64%
t_0	13.70	13.73	13.72	13.76	13.74	13.784	13.80	13.80

Description of parameter symbols and definitions are shown as follows:

H_o: Hubble constant (100h km/Mpc·s).

Ω_Λ: Dark energy density/Critical density.

Ω_m: Physical matter density Critical density.

Ω_b: Baryon density/Critical density.

Ω_c: Cold dark-matter density/Critical density.

t_0: Age of the Universe (Gyr).

From table 10, dark energy density Ω_Λ from 1-year WMAP results (2003) to Planck 2018 results for 15 years, the value from 73.22% decreases gradually down to 68.42%, decreasing 4.8%, but the total matter density Ω_m from 1-year WMAP results to Planck 2018 results, the value from 26.78% increases gradually up to 31.58%, increasing 4.8%. As the Universe expands rapidly, its temperature decreases and gradually cools, and then energy transforms into the building blocks of matter. The results show that dark energy transforms into matter at the same percentage of the Universe's content, which is consistent with the assertion of Big Bang theory.

The cosmological parameters of Planck 2018 results VI are taken as the current situation of the Universe. We may imagine that, at the first time of the Big Bang, the full energy (100% energy density) of the Universe gradually loses, after 13.8 billion years later, remains 68.42% energy density, which is dark energy density, and creates 31.58% total matter density. Therefore, we should take the current dark energy as "residual energy" of the Universe after the Big Bang.

5.2 The accelerating expansion of the Universe can be interpreted by multiverse

According to table 10, cold dark matter density Ω_c from the value of 22.34% at 1st-year WMAP increases gradually up to 26.64% at Planck satellite 2018, increasing 4.3%, and baryon density Ω_b in our cosmos from the value of 4.44% increases gradually up to 4.94%, only increasing 0.5%, which compares to the increasing rate of cold dark matter density Ω_c about 1：8.6. Temperature is a display of the thermal motion of microscopic particles; therefore, hot energy must display high temperatures and produces more particles after the Big Ban. In the table, the Ω_b increasing in value is so small that indicates energy in our cosmos so poor that we can call it a low-energy-density cosmos; on the contrary, Ω_c increasing in value is so large that indicates energy in other cosmoses than ours so much that we can call them the high-energy-density cosmoses. After the WMAP and Planck Satellite detecting, the current actual temperature of cosmic microwave background is 2.725 °K (Kelvin), which is very close to

absolute zero (0°K = −273.15℃); therefore, current energy of our low-energy-density cosmos is so poor that cannot contribute to an accelerating expansion of the Universe.

Under the 3-cosmic framework of the Universe, the rate of expansion in the high-energy-density cosmoses must be much higher than that of our low-energy-density cosmos. According to the property of fundamental interaction forces of nature, except gravitational force, the other fundamental forces cannot observe other cosmoses; therefore, the high-energy-density cosmoses cannot directly contribute to the accelerating expansion of our low-energy-density cosmos. However, when the high-energy-density cosmoses more rapidly expand than our low-energy-density cosmos, its matter (i.e., dark matter for our cosmos) will expand at the same pace, causing the effect of tugging the stars and galaxies of our low-energy-density cosmos at accelerating expansion, i.e., the effect of tugging stars and galaxies of the Universe at accelerating expansion in our view.

6. DISCUSSIONS

6.1 The quantum experiments indicate the existence of the multiverse in space

In classical physics, matter is made up of particles, which are entities that conform to a simple orbit and can calculate their motion, velocity, angle, and speed at any one time; for example, an elementary particle in atom ─ electron, in Newton's classical mechanics, rotates around the nucleus in a circular orbit, and the position, momentum, and orbit of each particle is fully predictable, and it is only in a single place at the same time. This idea is similar to the case in our solar system, but beginning in the 1920s, it is known from quantum experiments that in the atomic structure, quantum physicists tried to describe the “electrons” of the elementary particles accurately, they found that it were almost impossible, because it did not have a fixed position and the particles could indeed appear in different places at the same time, just as it has fractals, but when they actually look at it, they can only find it in one location. However, in quantum mechanics, the position and momentum of each elementary particle is expressed by a static, spherical wave function around the nucleus, which can only be counted by probability or statistics; in other words, the elementary particles do not in stable orbit, but intermittently appear in many places. The only explanation is that the particles not only exist in our cosmos, but also sweeps through other cosmoses, indicating the existence of multiple cosmoses in space, i.e., the multiverse exists.

In multiverse, among any other worlds, there is no basic interactive forces of nature except gravity, i.e., the graviton in the field of gravity can penetrate all the cosmoses, that is, gravity affects each other's orbits of stars, but electromagnetic forces (light) do nothing to each other, that is, the stars among the multiple cosmoses are invisible to each other. Since many compact objects of the other binary cosmoses cannot be seen, the phenomenon of gravity attraction among the triple cosmoses is the phenomenon of dark matter. So, dark matter may be situated

in the cosmoses other than ours; in other words, the multiverse can hold dark matters.

6.2 The existence of a dark planet X can solve problems of astronomical observation in solar system

In 1970s, Joseph Brady historically published records of the observation of Halley's Comet and found that its approach to the Sun has always been errors of 3 or 4 days in the predicted time of the perihelion passage. The prediction of Halley's Comet, Brady based on studies of periods of Halley's Comet using old European and Chinese records and used a computer to treat the data of it in a numerical model of the solar system. He has been able to predict an invisible X planet (trans-plutonian planet), affecting the orbit of Halley's Comet. It was about three times the size of Saturn, with highly inclined orbit ($i = 120°$, $e = \pm 0.07$) to the ecliptic and the period of it to be 450 years (Brady 1971, 1972).

In 1980s, scientists found that Uranus and Neptune were pulled off and deviated the normal orbit by an unknown force in the solar system; this unknown force may have come from an unknown planet, with its gravity disturbing these two giant planets. Flanders proposed a search for an X planet, which has about three times the mass of the Earth and a highly inclined eccentric orbit that accounted for all the perturbations on the motions of Neptune (Flandern 1981).

In 1988, NASA research scientist John Anderson, from observed astronomical data of the nineteen centuries presented the deviation of Neptune and Uranus in the regular orbit and proposed “The Theory of X Planet”. The mass of X planet is about five times that of the Earth and its period is about 700～1000 years. The orbit is elliptical and the inclination from the orbit to ecliptics large and almost perpendicular (Anderson 1988). Now the planet X has been searched for, but it remains to be found.

The Pioneer 10 and 11 spacecraft launched in 1973 and 1974 respectively, when the spacecrafts approached Neptune and Uranus, unknown objects were found that could affect their operations. In 2002, John Anderson and colleagues' previous analyses of radio Doppler and ranging data from distant spacecraft in the solar system indicated that an apparent anomalous acceleration is acting on Pioneer 10 and 11, with a magnitude about $8\times10-8$ cm/s2, directed towards the Sun. The effect is clearly significant and remains to be explained. Their tracking Pioneer 10 have assessed all known mechanisms and theories, but have so far found nothing, and cannot explain this Universe's mystical power; the probe has revealed an unknown force. The existing cosmology and space navigation theory will face a significant impact (Anderson et al. 2002).

in 2006, Pluto was reclassified as a dwarf planet, removing it from the count of major planets in our solar system. In 2016, astronomers proposed a Planet Nine based on the peculiar clustering of the orbits of several extreme trans-Neptunian objects (ETNOs) , which suggest a larger object is shepherding them. This gravitational influence suggests an unseen, massive planet in the distant outer solar system. The search for Planet Nine continues, as of 2024 the

semi-major axis of Planet Nine is estimated to be 290 ± 30 AU, this implies that the planet has an orbital period of 4,190 to 5,720 years, and has 4.4 ± 1.1 times the mass of the Earth [Siraj, Chyba & Tremaine 2025]. Astronomers use new observatories like the Vera C. Rubin Observatory to search Planet Nine, but there's no direct evidence yet.

If we consider a dark planet X or a dark Planet Nine, which orbits around the Sun in the other cosmos than ours, then its gravity will sometimes affect the motion of Halley's Comet, Neptune, Uranus, Pioneer 10 and 11 spacecrafts and the gravitational influence of ETNOs; therefore, the problem of the invisible object may be solved, and that can solve problems of astronomical observation in our solar system.

6.3 The interaction of dark matter and dark energy dominates the fate of the Universe

Scientists assume that dark energy is thought to be the force that tears apart the Universe, but the gravity of dark matter condenses everything, and the two forces mutual act on that dark matter and dark energy dominate the fate of the Universe and formed the structure of the Universe as we know today.

Energy causes the Universe expansion, because of its hot temperature, but matter makes each other's shrinkage because of the gravity; however, from the data of 2018 Planck results VI, current dark energy density 68.42% is bigger than total matter density 31.58% by 36.84%; therefore, this much dark energy certainly will accelerate the Universe rapid expansion.

As a result of the discovery of the 1a supernova, scientists speculate that the Universe continues to expand, and the speed is expanding faster and faster, and the structure of the space-time is unable to maintain the integrity of the Universe, making it colder and colder. Expansion keeps neighboring stars away and increasingly lonely, and becomes isolated star-and-planet, until the star's nuclear reactor runs out of fuel, tearing up the entire star system to the point where it tears up matter itself, and breaking the chemical bond, every atom of everything is torn apart, everything is broken down into elementary particles, leaving a dead-end remnant, and that is the end of the Universe — the **"**Big Rip**"** **[**Ellis et al. 2012]. Our Universe will eventually form an icy world of eternal complete silence, with no living thing to exist, and scientists estimate that it will take at least fifty billion years to happen. The Universe is expanding faster and faster, keeping galaxies farther apart, and is expected to tear the Universe apart, as if it were going to win the cosmic war.

The accelerating expansion of the Universe are different from "Dao", which came from a Chinese well-known philosopher Lao-tzu's "Dao De Jing" in the Spring and Autumn Period (about 2500 years ago). In chapter 25 of "Dao De Jing" described: **"**Something is blended, which is born peacefully and scarcely before the Universe appears, independent without change, revolving around without losing it and can be the mother of the world. I don't know its name, it is called **'**Dao**'**……, Man obeys the Earth, the Earth obeys Heaven, Heaven obeys Dao, Dao obeys Nature**"**. The regular way **"**Dao**"** of the Universe must also be revolved around without losing it; in other word, the regular way of the Universe must be revolved around to be able to

fit in and should not form an icy world that is forever dead, so scientists' presumption needs to be studied further.

On the other hand, according to the Big Bang Theory, dark energy will decrease gradually down, but total matter increases gradually up, when dark energy density decreases to below 50% or less, and total matter density increases to bigger than 50% or more, the Universe may stop to expand, and turn around to collapse in a **"**Big Crunch**"** due to the gravity.

7. CONCLUSION

From the conceptions of String theory, under the 3-cosmic framework of the Universe, triple cosmoses exist in space. A new study in a different view of the Earth's core was developed a new Earth model and used a simplification method to calculate the data of the Earth, then found a dark planet, which locates inside the Earth but in another cosmos than ours.

The current dark energy should be taken as the residual energy of the Universe after the Big Ban, and it is still in a high-energy state, so the high-energy-density cosmoses rapidly expand. Dark matter of the high-energy-density cosmoses should be subject to a "drag" on the stars and galaxies of our low-energy-density cosmos due to gravity, which causes the effect of pulling the accelerating expansion of the Universe in our view.

The 3-cosmic framework of the Universe should enable a new approach to breaking the bottleneck of research in the astrophysics of the Universe and geophysics of the Earth, but that still needs to be proved by the fine outcomes of physicists' new research.

REFERENCES

Ade, P. A. R. et al., Planck Collaboration. (2014). Planck 2013 results. I. Overview of the products and scientific results. *Astronomy & Astrophysics*, 571(A1), Table 10. Cosmological parameter values for the Planck-only best-fit 6-parameter ΛCDM model and for the Planck best-fit cosmology including external datasets, Planck (CMB + lensing), Best fit.

Ade, P.A.R. et al., Planck Collaboration. (2016). Planck 2015 results. XIII. Cosmological parameters. *Astronomy & Astrophysics*, 594(A13): 32, Table 4. Parameters of the base ΛCDM cosmology computed from the 2015 baseline Planck likelihoods (Planck TT+ low P).

Aghanim, N. et al., Planck Collaboration, (2020). Planck 2018 results. VI. Cosmological parameters. *Astronomy & Astrophysics*, 641(A6): 7, Table 1. Base-ΛCDM cosmological parameters from Planck TT, TE, EE + lowE + lensing, Plik best fit.

Agnew, D., Berger, J., Buland, R., Farrell, W. & Gilbert, F. (1976). International Deployment of Accelerometers: a network for very long period seismology, *EOS, Trαns. Am. Geophys. Union*, 57: 180–188.

Ahrens, T. J. (1980). Dynamic Compression of Earth Materials, *Science*, 207: 1035.

Alboussière, T., Deguen, R. & Melzani, M. (2010). Melting-induced stratification above the Earth's inner core due to convective translation. *Nature*, 466: 744-747.

Altshuler, L.V. & Sharipdzhanov, L. V. (1971). On the distribution of iron in the Earth, the chemical distribution of the latter. *Bull. Acad. Sci. USSR Geophys. Ser*. 4: 3-16.

Anzellini, S., Dewaele, A., Mezouar, M., Loubeyre, P. & Morard, G. (2013). Melting of Iron at Earth's Inner Core Boundary Based on Fast X-ray Diffraction, *Science*, 340 (6131): 464-466.

Bartusiak, Marcia. (1988). Wanted: Dark Matter, *Discover*, Dec. 1988. p. 63-69.

Bennett, C. L. et al. (1993). Scientific results from the Cosmic Background Explorer (COBE), *Proc Natl Acad Sci.* 1993 Jun 1;90 (11):4766–4773. https://doi.org/10.1073/pnas.90.11.4766

Bennett, C. L. et al. (2013). Nine-Year Wilkinson Microwave Anisotropy Probe (WMAP) Observations: Final Maps and Results. *The Astrophysical Journal Supplement Series*, 208(2): P.46, Table 17. Cosmological Parameter Summary (WMAP).

Bloxham, J. & Gubbins, D. (1987). Thermal core-mantle interactions. *Nature*, 325: 511-513.

Bloxham, J. & Jackson, A. (1990). Lateral temperature variations at the core-mantle boundary deduced from the magnetic field, *Physical Review Letters*, 17 (11): 1997-2000.

Boschi, L. & Dziewonski, A. M. (1999). High- and low- resolution images of the Earth's mantle: Implications of different approaches to tomographic modeling, *J. Geophys. Res.*, 104 (B11): 25567- 25594.

Boschi, L. & Dziewonski, A. M. (2000). Whole Earth tomography from delay times of P, PcP, and PKP phases lateral heterogeneities in the outer core or radial anisotropy in the mantle? *J. Geophys. Res.*, 105: 13675-13696.

Buchbinder, G. G. R. (1968). Properties of the Core-Mantle Boundary and Observations of PcP, *J. Geophys. Res*., 73: 5901.

Chandler, S. C. (1891). On the variation of latitude, *Astronomical Journal*, 11: 59–61, 65–70.

Condie, Kent C. (1997). Plate tectonics and crustal evolution (4th Ed.). *Butterworth-Heinemann*, p. 5.

Creager, K. C. & Jorden, T. H. (1986). A spherical structure of the core-mantle boundary from PKP travel time, *Geophysics. Res. Lett*., 13: 1497-1500.

Derr, J. S. (1969). Internal Structure of the Earth Inferred from Free Oscillations, *J. Geophysics. Res.*, 74: 5202-5220.

Deutsch, David. (2010). Apart from universes and many worlds, Everett, Quantum Theory and Reality, In S. Saunders; J. Barrett; A. Kent; D. Wallace (eds.), *Oxford University Press*. pp. 542-552.

Doornbos, D.J. & Hilton, T. (1989). Models of the core-mantle boundary and the travel times of internally reflected core phases, *J. Geophys. Res.*, 94 (B11): 15,741-15,751.

Dvali, G., (2004). Out of the Darkness, *Scientific American*, February 2004, 68-75.

Dziewonski, A.M. & Anderson, D. L. (1981). Preliminary Reference Earth Model, *Phsy. Earth Planet, Inter*., 25, 297-356.

Everett, Hugh. (1957). Relative State Formulation of Quantum Mechanics. *Reviews of Modern Physics*. 29, 454-462.

Forte, A. M. & Peltier, R. W. (1991). Mantle convection and core-mantle boundary topography: Explanations and implications, *Tectonophysics*, 187 (1-3): 91-116.

Garcia, R. & Souriau, A. (2000). Amplitude of the core-mantle boundary topography estimated by stochastic analysis of core phases. *Phys. Earth Planet. Inter.*, 117: 345-359.

Garland, G. D. (1979). Introduction to Geophysics (2nd ED.). *W. B. Saunders Company*, Toronto, Canada, 4–8, 28–30, 44–46, 130, 387–389.

Gross, Richard S. (2000). The Excitation of the Chandler Wobble, *Geophysical Research Letters*, 27 (15): 2329–2332.

Gubbins, D. & Richards, M. A. (1986). Coupling of the core dynamo and mantle: Thermal or Topography? *Physical Review Letters*, 13: 1521-1524.

Gubbins, D., Masters, T. G. & Nimmo, F. (2008). A thermochemical boundary layer at the base of Earth's outer core and independent estimate of core heat flux, *Geophys. J. Int.*, 174: 1007-1018.

Guth, Alan H. (1982). Fluctuation in the New inflationary, *Physical Review Letters*, Vol. 49, No. 15, pp.1110-1113.

Hall, T.H. & Murthy, V. R. (1972). Comments on the Chemical Structure of a Fe-Ni-S Core of the Earth, *EOS*. 53 (5): 602.

Hecht, J. (1995). Buried treasure from hot heart of the Earth. *New Scientist*, 19, 16.

Herndon, J. Marvin. (1993). Feasibility of a nuclear fission reactor at the center of the Earth as the energy source for the geomagnetic field, *Journal of Geomagnetism and Geoelectricity*, 45: 423–437.

Ho, Hsien-Jung. (1993). Reconstruction of the Earth Model and Discovery of the Interior Dark Matter, *The First Cross-Strait UFO Symposium*, On 7 December 1993 Beijing, China. https://doi.org/10.29924/REMDM.DB/Collection0001

Ho, Hsien-Jung. (2019). Based on the Space-Time of string Theory Exploring Dark Matter inside the Earth, *Journal of Scientific and Engineering Research*, 2019, 6 (8): 166-191. http://newidea.org.tw/pdf/S71.pdf

Ho, Hsien-Jung. (2022). The 3-Cosmic Framework of the Universe Can Hold Dark Matter and Dark Energy, *Journal of Scientific and Engineering Research*, 2022, 9 (4): 67–77. https://doi.org/10.5281/zenodo.10518988

Ho, Hsien-Jung. (2024). Dark Matter can be Revealed Inside the Earth by string Theory, *International Journal of Renewable Energy and Environmental Sustainability*, 2024, 9 (4): 1-28. https://doi.org/10.5281/zenodo.13982835
https://doi.org/10.3847/1538-4357/ad98f6

Jeanloz, R. & Ahrens, T. J. (1980). Equations of FeO and CaO, *Geophysics. J. R. Astr. Soc.*, 62: 505- 528.

Jeanloz, R. (1990). The Nature of the Earth's Core, *Annual Review of Earth and Planetary Sciences,* 18: 357-386.

Jephcoat, A. & Olson, P. (1987). Is the Inner Core of the Earth Pure Iron? *Nature*, 325: 332-335.

Kapteyn, Jacobus Cornelius. (1922). First attempt at a theory of the arrangement and motion of the sidereal system, *Astrophysical Journal*, 55: 302-327.

Kaula, W.M., Sleep, N.H. & Phillips, R.J. (1989). More about the Moment of Inertia of Mars, *Geophysical Research Letters*, 16 (11): 1333–1336.

Knopoff, F. (1965). A preeminent seismology, *Phys. Rev*., 138 (A): 1445.

Komatsu, E. et al. (2009). Five-Year Wilkinson Microwave Anisotropy Probe (WMAP) Observations: Cosmological Interpretation. *The Astrophysical Journal Supplement Series*, 180(2): 371, Table 14. Comparison of ΛCDM Parameters for WMAP+BAO+SN with Various SN Compilations, Union.

Komatsu, E. et al. (2011). Seven-Year Wilkinson Microwave Anisotropy Probe (WMAP) Observations: Cosmological Interpretation. *The Astrophysical Journal Supplement Series*, 192(2): 3, Table 1. Summary of the Cosmological Parameters of ΛCDM Model, WMAP+BAO+H0 Mean.

Kubala, Bizy, & Mahan Rao. (1996). Earth's Core Temperature. *Byrdand Black*.

Lay, T. (1989). Structure of the Core-Mantle Transition Zone: A Chemical and Thermal Boundary Layer, *EOS*, Jan., 70(4): 24, 49, 54-55, 58-59.

Leake, J. (2013). Cosmic map unveils first evidence of other universes, *The Sunday Times*, 19 May 2013.

Lemaître, Georges. (1927). Un Univers homogène de masse constante et de rayon croissant rendant compte de la vitesse radiale des nébuleuses extra-galactiques, *Annales de la Société Scientifique de Bruxelles*, A47, p. 49-59.
Lyttleton, R.A. (1973). The end of the iron-core age, *Moon*, 7: 422-439.
McFadden, Phillip L. & Merrill, R. T. (1995). History of Earth's magnetic field and possible connections to core-mantle boundary processes. *J. Geophys. Res.*, 100: 307-316.
McQueen, R. G., Marsh, S. P., Taylor, J. W., Fritz, J. N. & Carter, W. J. (1970). The equation of state of solids from shock wave studies, in high velocity impact phenomena, Kinslow, R., *Academic Press*, New York, 294-419.
Mersini-Houghton, Laura. (2008). Birth of the universe from the Multiverse, *Department of Physics and Astronomy, North Carolina University*, September 22, 2008.
Messling, N., Willbold, M., Kallas, L., Elliott, T., Fitton, J. G., Müller, T., & Geist, D. (2025). Ru and W isotope systematics in ocean island basalts reveals core leakage. *Nature*, 642, 376–380. https://doi.org/10.1038/s41586-025-09003-0
Morelli, A. & Dziewonski, M. (1987). Topography of the core-mantle boundary and lateral homogeneity of the liquid core, *Nature*, 325: 678–683.
Mundl, A. et al. (2017). Tungsten-182 heterogeneity in modern ocean island basalts. *Science*, 356, 66–69.
Mundl-Petermeier, A. et al. (2020). Anomalous 182W in high 3He/4He ocean island basalts: fingerprints of Earth's core? *Geochim. Cosmochim. Acta*, 271, 194–211.
Neuberg, J. & Wahr, J. (1991). Detailed investigation of a spot on the core mantle boundary using digital PcP data, *Phys. Earth planet. Inter.*, 68: 132-143.
Obayashi, M. & Fukao, Y. (1997). P and PcP travel time tomography for the core-mantle Boundary. *J. Geophys. Res.*, 102: 17825-17841.
Oort, Jan H. (1932). The force exerted by the stellar system in the direction perpendicular to the galactic plane and some related problems. *Bulletin of the Astronom. Inst*. The Netherlands, Vol. 6, p. 249-287.
Penzias, A. A. and Wilson, R.W. (1965). A Measurement of Excess Antenna Temperature at 4080 Mc/s. *Astrophysical Journal*, 142: p. 419-421.
Perlmutter, S. et al. (1999). Measurements of Ω and Λ from 42 High-Redshift Supernovae, *Astrophysical Journal*, Volume 517, Number 2, 517, 565-586.
Peterson, J., Butler, H. M., Holcomb, L. G. & Hutt, C. R. (1976). Seismic research observatory, *Bull. Seism. Soc. Am*. 66: 2049-2068.
Ramsey, W. H. (1948). On the constitution of the terrestrial planets, *Mon. Not. Roy. Astron. Soc*., 108: 406-413.
Riess, Adam G. et al. (1998). Observational Evidence from Supernovae for an Accelerating universe and a Cosmological Constant, *The Astronomical Journal*, Volume 116, Number 3, 116 1009.
Ringwood, A. E. (1984). The Earth's Core: its composition, formation and bearing upon the origin of the Earth, *Proc. R. Soc*. A, 395: 1-46.
Rizo, H. et al. (2019). 182W evidence for core-mantle interaction in the source of mantle plumes. *Geochem. Perspect. Lett.*, 11, 6–11.
Rodgers, A. & Wahr, J. (1993). Inference of core-mantle boundary topography from ISC PcP and PKP travel times. *Geophys. J. Int.* 115: 991-1011.
Rudnick, Lawrence; Shea Brown and Liliya R. Williams, (2007). Extragalactic Radio Sources and the WMAP Cold Spot, *The Astrophysical Journal*, Volume 671, Number 1, 40.
Ruff, L. & Anderson, D. L. (1980). Core formation, evolution, and convection: A geophysical model, *Phys. Earth Planet. Inter.*, 21**:** 181-201.
Scherk, Joel & Schwarz, John H. (1975). Dual field theory of quarks and gluons, *Physics Letters*, 57, B, 463-466.

Siegfried, T. (1999). Hidden Space Dimensions Can Permit Parallel Universes and Explain Cosmic Mysteries. *The Dallas Morning News*, 5 July 1999.

Siraj, Amir; Chyba, Christopher F.; Tremaine, Scott. (2025). "Orbit of a Possible Planet X". *The Astrophysical Journal*. 10 January 2025, 978 (2): 139.

Soldati, G., Boschi, L., Mora, S. D. & Forte, A. M. (2014). Tomography of core-mantle boundary and lowermost mantle coupled by geodynamics: joint models of shear and compressional velocity, *Annals of Geophysics,* 6: 57.

Soldati, G., Koelemeijer, P., Boschi, L. & Deuss, A. (2013). Constraints on core-mantle boundary topography from normal mode splitting: *Geochem. Geophys. Geosyst*. 14.

Spergel, D. N. et al. (2003). First Year Wilkinson Microwave Anisotropy Probe (WMAP) Observations: Determination of Cosmological Parameters. *The Astrophysical Journal Supplement Series*, 148(1): 192, Table 10. Basic and Derived Cosmological Parameters: Running Spectral Index Model.

Spergel, D.N. et al. (2007). Three-Year Wilkinson Microwave Anisotropy Probe (WMAP) Observations: Implications for Cosmology. *The Astrophysical Journal Supplement Series*, 170(2): 380, Table 2. Power-Law CDM Model Parameters and 68% Confidence Intervals, 3 Year + ALL Mean.

Stsrobinskii A. A. and Zel'dovich, Z. B. (1988). Quantum Effects in Cosmology, *Nature* 331, 25.

Susskind, L. (2006). Father of string Theory Muses on the Megaverse. *New York Academy of Science Publications*, April 14, 2006.

Sze, E.K.M. & van der Hilst, R. D. (2003). Core Mantle Boundary Topography from Short Period PcP, PKP and PKKP data, *Physics of the Earth and Planetary Interiors*, 135: 27-46.

Walker, R. J., Morgan, J. W. & Horan, M. F. (1995). Osmium-187 in some plumes: Evidence for core-mantle interaction? *Science*, 269, 819–822.

Woit, P. (2013). The "Dark Flow" & Existence of Other universes —New Claims of Hard Evidence, *New Scientist*, June 03, 2013.

Woodhouse, J. H. & Dziewonski, A. M. (1989). Seismic modeling of the Earth's large-scale three-dimensional structure, *Phil. Trans. R. Soc. Lond*. A 328, 291-308.Yoshida, M. (2008). Core-mantle boundary topography estimated from numerical simulations of instantaneous flow. *Geochem. Geophys. Geosys*. 9 (7).

Yoshida, M. (2008). Core–mantle boundary topography estimated from numerical simulations of instantaneous flow. Geochem. Geophys. Geosys., 9: 7.

Young, C. J. & Lay, T. (1987). The core-mantle boundary, *Ann. Rev. Earth Planet. Sci.*, 15: 25-46.

Zwicky, F. (1937). On the Masses of Nebulae and of Clusters of Nebulae. *Astrophysical Journal*, 86, 217.